Circulation response to aerosol forcing of the 1970s and 2000s - the case of the North Atlantic warming hole

S. Fiedler[1] and D. Putrasahan[2]

[1]University of Cologne, Institute for Geophysics and Meteorology, Cologne, Germany. Previously: Max-Planck-Institute for Meteorology, Atmosphere in the Earth System, Hamburg, Germany.
[2]Max-Planck-Institute for Meteorology, Ocean in the Earth System, Hamburg, Germany.

Key Points:

- Anthropogenic aerosol patterns affect dynamical processes in the atmosphere and ocean
- Aerosol pattern change from 1970s to 2000s enhance North Atlantic warming hole and Arctic temperatures
- Most of the temperature response is associated with the anthropogenic aerosol effect on clouds

Corresponding author: Stephanie Fiedler, `stephanie.fiedler@uni-koeln.de`

Abstract

We show how changes in the global distribution of anthropogenic aerosols favour different spatial patterns in the North Atlantic sea-surface temperature (NASST). The NASSTs largely show the expected decrease associated with the anthropogenic aerosols in the 1970s, but also a surprising warming response in the eastern sub-polar gyre, the region of the North Atlantic warming hole. The NASST response reversed for the anthropogenic aerosols in the 2000s against 1970s. The regional reduction in anthropogenic aerosols favoured (1) a strengthening of the warming hole and (2) a NASST increase at high latitudes associated with changes in the atmosphere-ocean dynamics. The gyre component of the northward Atlantic heat transport in mid- to high latitudes is an important driving mechanism. At least two-thirds of the NASST response is associated with the magnitude of aerosol-cloud interactions. Constraining the NASST response therefore depends on a better understanding of the uncertain aerosol effects on clouds.

1 Introduction

Patterns in the North Atlantic sea-surface temperature (NASST) change over time. Observations indicate a clear change from negative NASST anomalies in the 1970s to 1990s to positive anomalies in more recent decades (Enfield et al., 2001; Trenberth & Shea, 2006), superimposed on the positive global trend in NASSTs associated with the increase in atmospheric greenhouse gas concentrations (IPCC, 2013). We illustrate the global pattern of NASST differences with results from the historical simulations of the Max Planck Institute - Earth System Model (MPI-ESM1.2; Fig. S1), using transient changes in atmospheric composition of the Coupled Model Inter-comparison Project phase six (CMIP6, Eyring et al., 2016). While most ocean regions show the expected warming due to greenhouse gas forcing since the pre-industrial, the sub-polar gyre in the North Atlantic stands out with a cool anomaly, referred to as the warming hole. Relative to the 1970s, this warming hole changed little while the northern hemisphere in the 2000s generally warmed more than the southern hemisphere. Despite the importance of understanding near-surface warming patterns, the underlying physical mechanisms of NASST pattern changes are still poorly understood, so much so that different plausible explanations exist (e.g., Delworth & Mann, 2000; Otterå et al., 2010; Booth et al., 2012; Wang et al., 2012; Clement et al., 2015; Kim et al., 2018; Keil et al., 2020).

Booth et al. (2012) proposed that the reduction of anthropogenic aerosol concentrations over the North Atlantic plays a role in reproducing the temperature changes with their CMIP5 model HadGEM2-ES. Anthropogenic aerosols reduce the incoming shortwave radiation at the surface through scattering and absorption, termed aerosol radiation interaction (ARI), as well as through aerosol effects on clouds, known as aerosol-cloud interaction (ACI). The magnitude of the associated radiative forcing is much debated, but an agreement is that the uncertainty in ARI is smaller than in ACI (Bellouin et al., 2020). The lower anthropogenic aerosol optical depth (τ_a) over the North Atlantic in the 2000s (Fig. 1a) is associated with less incoming shortwave radiation being scattered back to space compared to the 1970s. The less negative radiative effects in the 2000s relative to the 1970s over the North Atlantic (Fig. 1b) suggest an accelerated warming during this period. For instance, temperature observations over land support such an accelerated warming since the 1970s, following a multi-decadal period of global dimming by anthropogenic aerosols until the 1970s associated with a weaker warming (Wild, 2009).

This idea of changes in NASST patterns being a forced response to anthropogenic aerosol forcing (Booth et al., 2012; Bellucci et al., 2017) seems at odds with another scientific perception, namely that natural variability internal to the system drives NASST anomalies. One example is the study by Delworth and Mann (2000) identifying NASST anomalies much earlier in the history with data of the past 330 years. Since part of this data includes the pre-industrial era when anthropogenic aerosol burden was much lower

than today, it suggests that anthropogenic aerosol changes alone can not be the full explanation of changes in NASST patterns. However, this does not preclude to anthropogenic aerosol not having an influence on ocean dynamics and consequently, NASST patterns. Past studies linked changes in the NASST pattern with differences in the Atlantic Meridional Overturning Circulation (AMOC, e.g., Delworth & Mann, 2000; Drijfhout et al., 2012; Knight et al., 2005). When the AMOC is relatively strong, the North Atlantic becomes anomalously warm due to a stronger northward heat transport, corresponding with a warm phase of the North Atlantic. In response of the positive SST anomaly in the polar North Atlantic, ocean convection reduces and leads to a subsequent weakening of the AMOC. Since now less heat is transported northwards, a cool phase of the North Atlantic develops (e.g., Zhang & Wang, 2013; Knight et al., 2005).

In light of these two seemingly different explanations for the drivers of NASST patterns, we here revisit the response of NASSTs to anthropogenic aerosol changes of the 1970s and 2000s in order to reconcile the different perspectives. The two general ideas outlined aloft are not new, but we give a first systematic assessment of the NASST response to anthropogenic aerosols and explain the surprising behaviour in the North Atlantic warming hole. To this end we consider model-internal variability, give particular attention to the current uncertainty in the magnitude of anthropogenic aerosol radiative forcing, and assess the counter-intuitive response in the warming hole at the level of dynamical processes. Our study is guided by the following hypotheses:

1. *The anthropogenic aerosol pattern of the 1970s leads to a stronger cooling response in the North Atlantic than the aerosols of the 2000s.* We expected it due to the more negative radiative effects for the 1970s over the North Atlantic in five contemporary climate models (Fiedler et al., 2019a) and the paradigm change from global dimming to brightening in observations paired with an accelerated warming (Wild, 2009; IPCC, 2013).
2. *Uncertainty in ACI dominate the strength in the NASST response.* This is motivated by the model spread in the magnitude of ACI that is larger than the one for ARI (Bellouin et al., 2020) and the case of the CMIP5 model HadGEM2-ES (Booth et al., 2012). HadGEM2-ES has a relatively strong radiative forcing of anthropogenic aerosols (Bellouin et al., 2011) and has been used to argue that the historical forcing of anthropogenic aerosols is important for reconstructing the development of NASSTs (Booth et al., 2012).
3. *Dynamical processes in both atmosphere and ocean influence the NASST response to anthropogenic aerosol.* We postulate that anthropogenic aerosols can exert an influence on both the atmosphere and ocean, for which the ocean response can superimpose on naturally-occurring oceanic drivers of NASST. The hypothesis is based on competing theories about the origins of NASST variability in past studies and the identification of NASST anomalies in the pre-industrial era (e.g., Delworth & Mann, 2000; Booth et al., 2012; Clement et al., 2015; Kim et al., 2018), when τ_a was low and is therefore eliminated as sole driver of NASST anomalies.

We introduce the experiment strategy to test the hypotheses in Section 2, followed by the results (Section 3) and their discussion (Section 4), and draw conclusions at the end (Section 5).

2 Experiment strategy

We perform a suite of experiments using the CMIP6 configuration of MPI-ESM1.2 (Mauritsen et al., 2019). A main difference between MPI-ESM1.2 and previous model versions is the implementation of the novel simple plumes parameterization, MACv2-SP (Fiedler et al., 2017; Stevens et al., 2017), for optical properties of anthropogenic aerosols and an associated effect on the cloud albedo. Comprehensive evaluations of MPI-ESM1.2

against observations and other climate models have previously been conducted (e.g., Fiedler et al., 2019a; Maher et al., 2019; Mauritsen et al., 2019).

We perform five simulations (Table 1) with each integrated for 250 years to reduce the impact of model-internal variability on the magnitude of the SST response. Each experiment setup uses the same initial and annually repeating boundary data, except for the anthropogenic aerosols. Experiment PI has no anthropogenic aerosol and is our pre-industrial (1850) reference simulation. All other experiments use prescribed annually repeating monthly means of anthropogenic aerosol optical properties and an associated effect on the cloud albedo (Twomey effect) from MACv2-SP. Briefly, SP-05 uses the values for the 2005 and SP-75 for the 1975 with further details on MACv2-SP explained elsewhere Fiedler et al. (2017); Stevens et al. (2017). The different τ_a patterns in SP-75 and SP-05 (Fig. 1a−b) imply roughly a τ_a reduction by a factor of 2 over the North Atlantic, thus regionally $\tau_a(1970s) \approx 2\tau_a(2000s)$.

We additionally perform two simulations for further diagnostics for the 1970s aerosol. Firstly, this is experiment SP-75-NT, where we switch off ACI and simulate ARI only. We do so by prescribing the anthropogenic aerosol optical properties of 1975, but do not perturb the cloud droplet number concentrations, i.e., we use identical cloud droplet number concentrations as for PI. By comparison to SP-75, we separate the contributions from ACI (SP-75 minus SP-75-NT) and ARI (SP-75-NT) to the climate response. Secondly, we perform simulation SP-75-ATF, where we roughly quadrupled τ_a and the associated Twomey effect. Technically, we quadruple τ_a in the plume centers of the 1970s pattern that scales the global distribution of τ_a and the associated Twomey effect. In essence, we obtain a stronger radiative forcing without changing the spatial pattern to gain additional confidence in our results for the contributing mechanisms, since the response in SP-75 and SP-75-ATF is qualitatively similar (not shown). The response to anthropogenic aerosol changes are determined by calculating the difference in the mean state of the simulations. The first 50 (100) years are removed as spin-up period before analysing the climate (AMOC) response.

3 Results

3.1 Global mean SST

While there are substantial differences in the global distribution of anthropogenic aerosols in the 1970s and 2000s, surprisingly, the global mean SST response in the two periods are very similar, with a cooling by -0.18°C relative to PI. The magnitude of ACI is crucial to constrain the global mean SST response. We estimate that ACI explains more than two third of the global mean SST response to anthropogenic aerosols in our model (Table 1; SP-75 vs. SP-75-NT), despite our radiative forcing of anthropogenic aerosols associated with ACI (Fiedler et al., 2017) being relatively smaller compared to other contemporary estimates (Bellouin et al., 2020; Gryspeerdt et al., 2020). Inducing stronger aerosol effects on clouds would therefore efficiently reduce the global mean SST, all else held constant. A stronger cooling associated with potentially stronger ACI is not implausible in light of the uncertainty (Bellouin et al., 2020) and could for instance be expected in EC-Earth, which has a more negative aerosol forcing due to the stronger ACI with MACv2-SP (Fiedler et al., 2019a).

3.2 SST pattern

The negative anthropogenic aerosol radiative effects (Fig. S2) causes the expected northern hemisphere SST reduction in SP-75 compared to PI, but the eastern part of sub-polar gyre in the North Atlantic responds with a SST increase (Fig. 1c). Regional SST reductions associated with anthropogenic aerosols are at the order of -0.5°C. In the sub-polar gyre, the SST is higher in SP-75 compared to PI by about the same magni-

tude, despite the negative radiative forcing of the prescribed anthropogenic aerosols (Fiedler et al., 2019a). This result is surprising in the sense that adding aerosols is expected to scatter more incoming shortwave radiation and hence to cool the surface. This is clearly not the case over the sub-polar gyre.

The mean NASST responses for the 2000s aerosol pattern is similar, with a spatially averaged NASST response of -0.28°C in SP-75 and -0.27°C in SP-05 relative to PI (Table 1). However, the spatial patterns of the NASST response differ between SP-75 and SP-05 (Fig. 1d). The NASST in polar regions is higher in SP-05 than in SP-75, suggesting that the 1970s to 2000s reduction in τ_a over the Atlantic has contributed to Arctic amplification. The smaller τ_a over the North Atlantic in SP-05 is associated with weaker outgoing shortwave radiation favouring a relative warming compared to SP-75 in synergy with the effect of increasing greenhouse gas emissions. Again, the SST in the eastern sub-polar gyre behaves opposite to what would be expected from the regionally reduced τ_a. This is a clear warming hole identified in the eastern sub-polar gyre in SP-05 relative to SP-75.

The presence of a North Atlantic warming hole is consistent with observations (e.g., Drijfhout et al., 2012; Rahmstorf et al., 2015; Gervais et al., 2018). Our experiments indicate that the regional reduction in anthropogenic aerosol burden since the 1970s to 2000s contributed to the strengthening of the warming hole, namely with a regional maximum in cooling of about -0.5°C. A role of anthropogenic aerosol for the warming hole might seem counter-intuitive for such a development at first sight, since the regional pollution has been reduced and therefore suggests a warming. Indeed, the radiative forcing over the North Atlantic in SP-05 is less negative than in SP-75 (Fiedler et al., 2017) and can therefore not be the direct driver of the warming hole. The regional reduction in anthropogenic aerosol rather induces responses of the atmosphere and ocean dynamics that explain the behaviour in the warming hole, which we assess next.

3.3 Atmospheric dynamics

3.3.1 Near-surface conditions

We identify responses of the atmospheric conditions near the surface. Here, we use SP-75-ATF that has the same aerosol pattern and qualitatively shows the same responses as SP-75 (not shown), but produces stronger signals for an easier identification. Note that the aerosol effects could also be larger than we prescribe in SP-75 because of the uncertainty in ACI. We revisit this aspect in Section 4.

Our analysis points to an increase in the zonal wind speed at 10 m across parts of the North Atlantic for SP-75-ATF relative to PI (Fig. 1e). This behaviour is particularly pronounced in northern hemisphere winter and consistent with the equatorward shift of the jet with larger τ_a over the North Atlantic (Fig. S3–S4). The 10m-wind response is also consistent with the increased horizontal pressure gradients, e.g., between the stronger Azores High and Icelandic Low, again particularly in northern hemisphere winter (Fig. 1f, S4). The response in the mean sea-level pressure is associated with the response of the vertical temperature profiles to the aerosol patterns (not shown). The weaker warming hole over the eastern subpolar gyre for higher τ_a is associated with anomalously low sea-level pressure. As a result, the horizontal pressure gradient between the Azores and higher latitudes increases inducing stronger zonal winds. This in turn affects the divergence of the northward Atlantic heat transport (NAHT) and thus the NASST distribution, which we discuss next.

3.4 Ocean dynamics

3.4.1 Atlantic meridional overturning circulation (AMOC)

The SST response indicates a change in ocean dynamics. Both τ_a distributions from the 1970s and 2000s are associated with a stronger AMOC, shown in Figure 2a−b. The change in the magnitude of the AMOC is up to 0.4 Sv and falls within the internal variability (Fig. 2a), but this does not necessarily imply that the effect of anthropogenic aerosols is negligible. It is not implausible that aerosol radiative effects, particularly ACI, could be stronger than in MPI-ESM1.2 (Fiedler et al., 2019a; Bellouin et al., 2020; Gryspeerdt et al., 2020). More negative aerosol radiative effects are expected to induce a stronger AMOC response. Take for instance the case of quadrupling aerosol radiative forcing (SP-75-ATF), where the AMOC in MPI-ESM1.2 strengthens beyond the model-internal variability (Fig. 2a). This suggests that AMOC can indeed respond to aerosol forcing, consistent with (Booth et al., 2012).

3.4.2 Northward Atlantic heat transport (NAHT)

The change in the NAHT explains the regionally different response of the NASST to the aerosol patterns, particularly the counter-intuitive behaviour of the North Atlantic warming hole. For a detailed analysis, we decompose the total NAHT into the overturning and gyre components using an established method (e.g., Jungclaus et al., 2014) and illustrate them in Fig. 2c−e. At lower latitudes, up to roughly 40°N, the overturning component dominates the NAHT (Fig. 2c). At higher latitudes, the gyre component plays a larger role in the NAHT. Similar to the AMOC, NAHT is generally stronger in both SP-75 and SP-05 compared to PI (Fig. 2d) at lower latitudes where the overturning component of the NAHT dominates. Around 37°N, SP-75 has a marked maximum difference in NAHT of 20 TW compared to PI (blue solid line in Fig. 2d). It occurs right around where the difference in the gyre component (blue dotted lined) and difference in the overturning component (blue dashed line) intersect and namely follows the shape of the gyre component. This behaviour is associated with a relative convergence in NAHT that peaks around 40°N and extends to almost 60°N (blue solid line in Fig. 2e), and similarly is dominated by the gyre component. This regional convergence of heat is consistent with the warming in the eastern sub-polar gyre for SP-75 relative to PI.

The largest difference in the NAHT between SP-05 and SP-75 is again primarily explained by the gyre heat transport (brown lines Fig. 2d). Convergence in NAHT is much weaker in SP-05 compared to SP-75, leading to a relative divergence in NAHT around 40°N (solid red line in Fig. 2e) that is dominated by the gyre component (dotted red line), and therefore explains the cool anomaly in the eastern sub-polar gyre (Fig. 1d). Essentially, the net heat convergence (divergence) explains the positive (negative) NASST anomaly in the eastern sub-polar gyre, in contrast to the cooling (warming) elsewhere in the oceans on the northern hemisphere associated with the changes of the anthropogenic aerosols (Fig. 1c−d). Taken together, the sub-polar gyre circulation also contributes to the regionally different NASST response to the anthropogenic aerosols, in addition to the AMOC that is a more important contributor than the gyre for the northward heat transport at low latitudes.

4 Discussion

4.1 Contributions of dynamical processes

Our results indicate that anthropogenic aerosols of the 1970s and its evolution through to the 2000s influence the NASST patterns. The radiative effects of anthropogenic aerosols do so by inducing changes in the atmosphere and ocean dynamics. Figure 3 provides a conceptual view of the physical mechanisms governing the response of the NASST pat-

tern to the aerosols of the 1970s and 2000s. The increase in anthropogenic aerosols of the 1970s relative to PI induced lower NASST by both ARI and ACI, with ACI accounting for more than two-thirds of the reduction in NASST. Relatively lower NASST particularly over high latitudes like the Labrador Sea and the Greenland, Iceland and Norwegian (GIN) seas can induce more convection and thus increase the AMOC like diagnosed from our experiments. This increase in the AMOC aligns with the increased NAHT at lower latitudes like the subtropical North Atlantic.

We give evidence to reconcile the counter-intuitive response of the warming hole to aerosol patterns by analysing the NASST response in conjunction with the dynamics of the coupled atmosphere-ocean system. The analysis shows that the response of the NAHT explains the regional anomaly in the North Atlantic warming hole, primarily via differences in the divergence of the heat transport associated with the gyre component at high latitudes. In the warming hole region, we identify relatively higher SSTs for the 1970s aerosol relative to PI, even though the direct effect of anthropogenic aerosols is expected to reduce SSTs. This rather peculiar response in the gyre is explained by anomalous convergence of NAHT at subpolar latitudes. This result points to a multi-decadal muting of the North Atlantic temperature response during high aerosol burden over the North Atlantic. The associated NAHT convergence in the sub-polar gyre counteracted the emergence of a warming hole that one would expect from the increasing greenhouse gas concentrations (Keil et al., 2020).

When anthropogenic aerosol subsequently reduced from the 1970s to the 2000s, NASST relatively increased, again with the exception of the warming hole region. Our results indicate that the NAHT over this region was anomalously divergent and thus strengthened the warming hole through anomalously lower SSTs for the 2000s relative to the 1970s. The response of the warming hole for the 2000s against 1970s in our coupled experiments is consistent with results from atmosphere-only experiments for a future climate by Gervais et al. (2019).

4.2 Role of uncertainty in aerosol forcing

All our experiments show variability in NASSTs independent of the presence of anthropogenic aerosols, but the mean climate response to the aerosol radiative effects indicates a contribution of the anthropogenic aerosol changes to the NASST patterns. The question arises how strong this contribution is. For instance, Booth et al. (2012) showed a stronger NASST response to anthropogenic aerosol changes than our model simulations. We find increases in the AMOC scaling with the magnitude of the anthropogenic aerosol forcing. The AMOC increase with more aerosols is in line with the idea that the general circulation acts to weaken the larger latitudinal temperature differences, here induced by ARI and ACI. Our AMOC response falls within (outside) the typical model-internal variability of the AMOC, when the radiative effects of anthropogenic aerosols are closer to the upper (lower) bound of the spread in aerosol radiative forcing.

The uncertainty in the radiative forcing of anthropogenic aerosols translates to an uncertainty in the SST response. The CMIP5 model used by (Booth et al., 2012) has a stronger anthropogenic aerosol forcing (Bellouin et al., 2011) than our CMIP6 model (Fiedler et al., 2017). Both model estimates fall within the current uncertainty for the aerosol radiative forcing (Bellouin et al., 2020). We perceive the results by Booth et al. (2012) as an estimate at the upper end of the range of responses to plausible aerosol forcing magnitudes, whereas our results should be interpreted as an estimate towards the lower bound of plausible responses to anthropogenic aerosols. We identify in our simulations a dominant contribution of the aerosol effects on clouds (ACI) to the NASST response. Namely about two thirds of our NASST response is associated with ACI (Table 1), the magnitude of which is still uncertain (Bellouin et al., 2020).

5 Conclusions

We conducted 250-year long experiments with the coupled atmosphere-ocean model MPI-ESM1.2 with annually repeating aerosol properties of the 1970s and 2000s. Our results do not allow to reject the hypotheses outlined in the introduction and lead to the following conclusions:

- At least two-thirds of the global mean SST response to anthropogenic aerosols is associated with the magnitude of aerosol-cloud interactions. The degree to which aerosols and clouds interact therefore significantly contributes to the NASST response.
- For most of the North Atlantic, the response to the increased anthropogenic aerosols in the 1970s is a decrease of the NASST and a relative NASST increase from the 1970s to 2000s when aerosol burden was reduced. These findings are qualitatively consistent with earlier studies (Booth et al., 2012; Wild, 2009).
- In the eastern subpolar gyre, the behaviour is opposite to the rest of the North Atlantic. This is a warm anomaly for the 1970s aerosol pattern compared to the pre-industrial, indicating a muting of the warming hole, when taken together with the response to greenhouse gas concentrations (Keil et al., 2020). The anthropogenic aerosol reduction from the 1970s to 2000s is associated with a cool anomaly, thus favours a strengthening of North Atlantic warming hole. Our process analysis points to an anomalous NAHT convergence (divergence) arising from the gyre transport causing this response to the 1970s (2000s) aerosol pattern.
- We identify a dynamical response of the fully coupled ocean-atmosphere system to changes in the aerosol pattern. In conjunction with the response of NASST and the North Atlantic warming hole to increased aerosol loading, we diagnosed a consistent response of atmospheric circulation. That is an increase in the horizontal gradient in the mean sea-level pressure, stronger near-surface zonal winds, and a latitudinal shift in upper-tropospheric jetstream over the North Atlantic.
- More negative aerosol radiative effects are associated with a stronger AMOC. Qualitatively, our findings suggest that a continued global reduction of anthropogenic aerosols, e.g., as future emission of CMIP6 suggest (Fiedler et al., 2019b), would favour a decrease of the AMOC and a stronger warming hole signal, all else being equal.

We argued that the magnitude of the NASST pattern response to aerosol changes largely depends on the still poorly constrained aerosol effects on clouds. This implies that uncertainty in the radiative effects of aerosols translates to a loosely constrained response of NASSTs, as well as the response of the ocean and atmosphere. This includes for instance the mean position of the jetstream over the North Atlantic, which differs across climate models (e.g., Zappa et al., 2013).

Future studies should systematically quantify the model spread for the warming hole using transient simulations with well quantified radiative forcing of atmospheric composition changes. Such simulations are increasingly available from the "Radiative Forcing Model Intercomparison Project" (RFMIP, Pincus et al., 2016) and the "Detection and Attribution Model Intercomparison Project" (DAMIP, Gillett et al., 2016). Contrasting the warming hole of the 1970s and 2000s in these models and observations has the potential to test the plausibility of the aerosol radiative effects in the models.

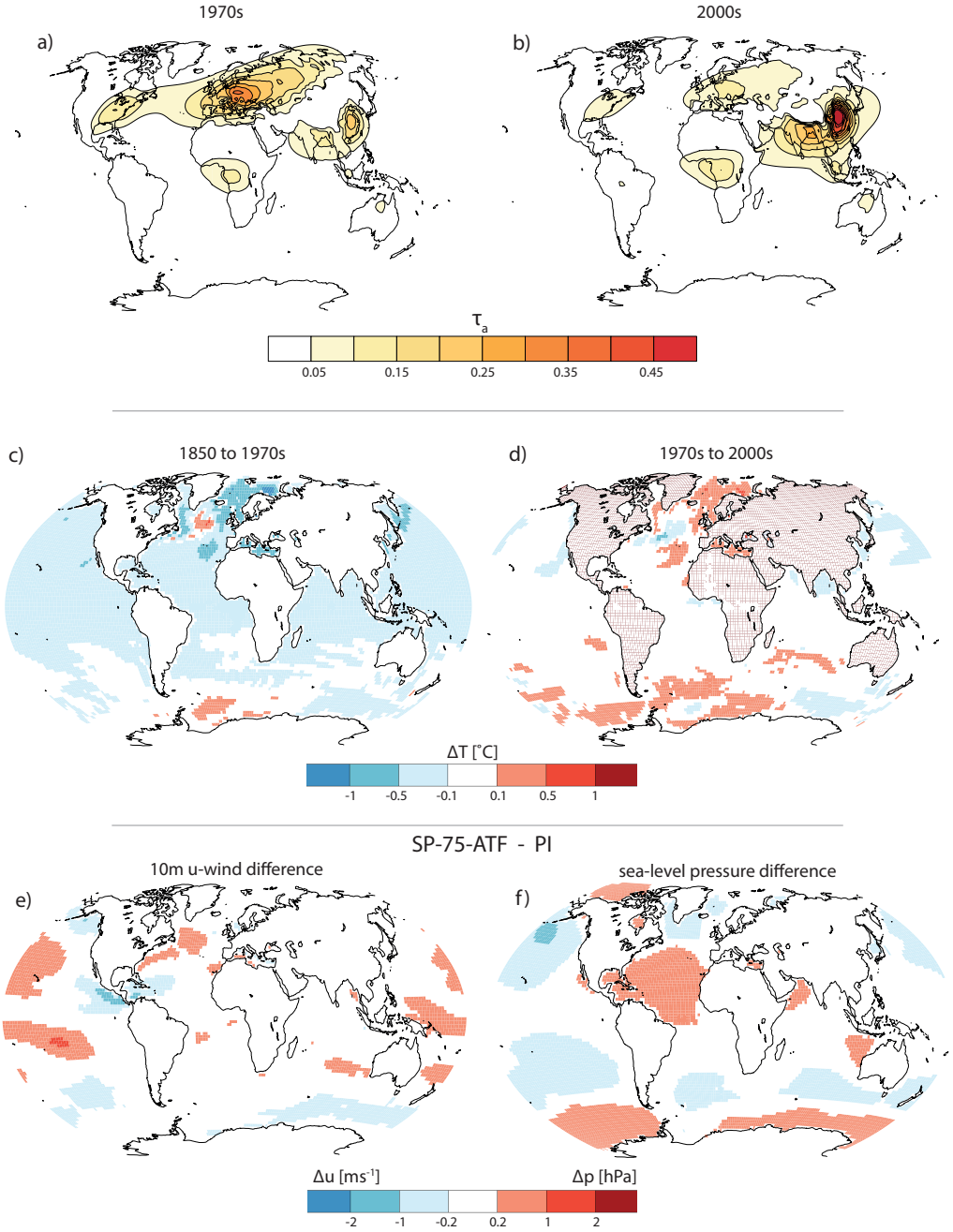

Figure 1. Anthropogenic aerosol optical depth and climate response. Shown are the mean anthropogenic aerosol optical depth (τ_a) for the (a) 1970s and (b) 2000s, the response of the climatological mean sea-surface temperature (ΔT) to τ_a of (c) the 1970s (SP-75) against 1850 (PI) and (d) the 2000s (SP-05) against the 1970s (SP-75), as well as the response of (e) the zonal wind component at 10 m (Δu) and (f) the mean sea-level pressure (Δp) to the 1970s aerosol pattern with enhanced τ_a (SP-75-ATF) compared to 1850 (PI). Results are based on 200-years of model output that account for aerosol-radiation interaction, the Twomey effect, rapid adjustments, and slow responses.

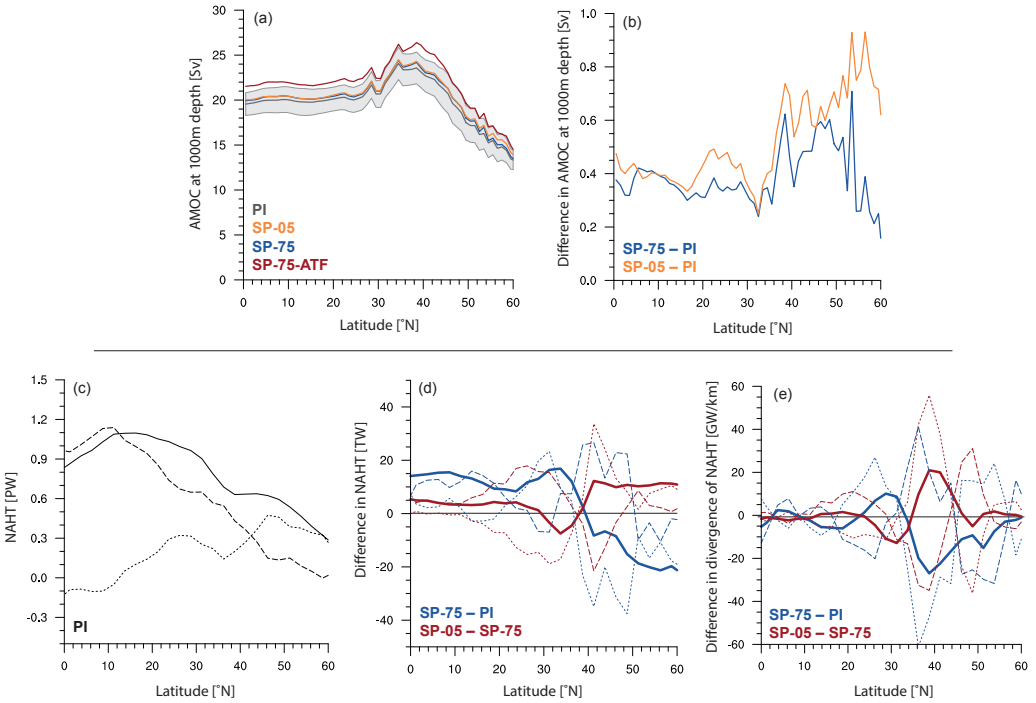

Figure 2. Response of the North Atlantic ocean dynamics to anthropogenic aerosol. Shown is the response of (a–b) the Atlantic meridional overturning circulation (AMOC) at 1000 m below the sea surface, and (c–e) the northward Atlantic heat transport (NAHT) separated into gyre (dotted) and overturning (dashed) components as (c) absolute values for PI, (d) absolute differences, and (e) differences in the divergence. The calculation of the divergence is based on NAHT data regressed onto 3rd order polynomials to smooth variations over length scales shorter than 800 km using a filter (Savitzky & Golay, 1964).

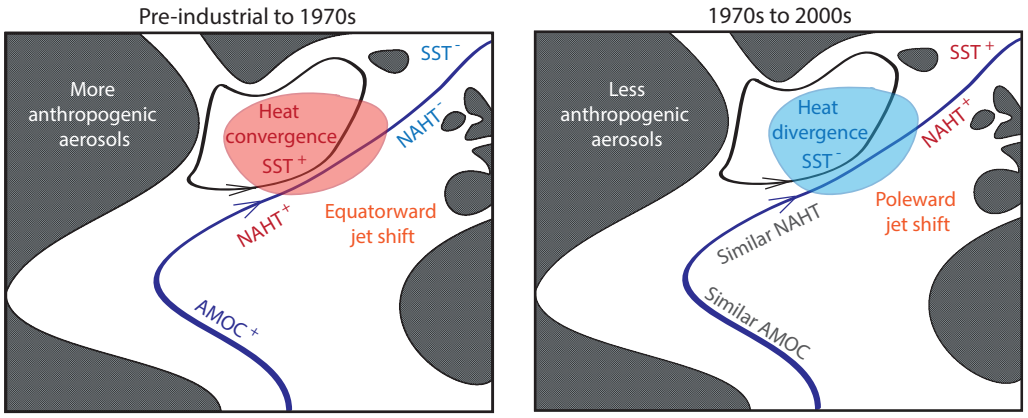

Figure 3. Sketch of the sea-surface temperature (SST) response to the different patterns of anthropogenic aerosols. The left (right) depicts the decrease (increase) in NASST for the 1970s (2000s) opposite to the weakening (strengthening) of the warming hole. The differences in the Atlantic Meridional Overturning Circulation (AMOC), and the Northward Atlantic Heat Transport (NAHT) are indicated. Blue line indicates the AMOC, black circular line the sub-polar gyre circulation, and dark shading land.

Table 1. Overview on model experiments (a)

	Experiment setup		Global Oceans			North Atlantic		
Name	t_{ARI}	t_{ACI}	τ_a	F [Wm^{-2}]	ΔT [°C]	τ_a	F [Wm^{-2}]	ΔT [°C]
PI	1850	1850	0	0	0	0	0	0
SP-05	2005	2005	0.01	-0.36	-0.18	0.02	-0.84	-0.27
SP-75	1975	1975	0.01	-0.31	-0.18	0.04	-1.42	-0.28
SP-75-NT	1975	1850	0.01	-0.06	-0.05	0.04	-0.43	-0.09
SP-75-ATF	1975*	1975*	0.03	-0.55	-0.26	0.18	-3.38	-0.54

(a) Listed are the chosen years for the aerosol-radiation interaction (t_{ARI}) and aerosol-cloud interaction (t_{ACI}) in MACv2-SP as well as the anthropogenic aerosol optical depth (τ_a), the equilibrium radiative forcing (F) and the SST response (ΔSST) averaged over global oceans and the North Atlantic (80°W−0°, 0°−60°N). * marks larger τ_a, but identical spatial distribution as of the year 1975.

Acknowledgments

This work was funded by the Max Planck Society. We are grateful for the liberty to collaborate on this inter-disciplinary research project in atmospheric sciences and oceanography at MPI-M. Moreover, we acknowledge the usage of the DKRZ supercomputer for performing the simulations with MPI-ESM1.2. We thank Samira Terzenbach, Karl-Hermann Wieners, and Helmuth Haak for technical support of this study. Information on the primary data including code access and model setup are given in the supplementary material.

References

Bellouin, N., Quaas, J., Gryspeerdt, E., Kinne, S., Stier, P., Watson-Parris, D., ... Stevens, B. (2020). Bounding global aerosol radiative forcing of climate change. *Reviews of Geophysics*, *58*(1), e2019RG000660. Retrieved from `https://agupubs.onlinelibrary.wiley.com/doi/abs/10.1029/2019RG000660` doi: 10.1029/2019RG000660

Bellouin, N., Rae, J., Jones, A., Johnson, C., Haywood, J., & Boucher, O. (2011). Aerosol forcing in the Climate Model Intercomparison Project (CMIP5) simulations by HadGEM2-ES and the role of ammonium nitrate. *J. Geophys. Res*, *116*, D20206. doi: 10.1029/2011JD016074

Bellucci, A., Mariotti, A., & Gualdi, S. (2017). The Role of Forcings in the Twentieth-Century North Atlantic Multidecadal Variability: The 1940–75 North Atlantic Cooling Case Study. *Journal of Climate*, *30*(18), 7317–7337. doi: 10.1175/JCLI-D-16-0301.1

Booth, B. B. B., Dunstone, N. J., Halloran, P. R., Andrews, T., & Bellouin, N. (2012, 04 04). Aerosols implicated as a prime driver of twentieth-century North Atlantic climate variability. *Nature*, *484*. doi: 10.1038/nature10946

Clement, A., Bellomo, K., Murphy, L. N., Cane, M. A., Mauritsen, T., Rädel, G., & Stevens, B. (2015). The Atlantic Multidecadal Oscillation without a role for ocean circulation. *Science*, *350*(6258), 320–324. doi: 10.1126/science.aab3980

Delworth, T. L., & Mann, M. E. (2000, Sep 01). Observed and simulated multidecadal variability in the Northern Hemisphere. *Climate Dynamics*, *16*(9), 661–676. doi: 10.1007/s003820000075

Drijfhout, S., van Oldenborgh, G. J., & Cimatoribus, A. (2012). Is a Decline of AMOC Causing the Warming Hole above the North Atlantic in Observed and Modeled Warming Patterns? *Journal of Climate*, *25*(24), 8373-8379. doi: 10.1175/JCLI-D-12-00490.1

Enfield, D. B., Mestas-Nuñez, A. M., & Trimble, P. J. (2001). The Atlantic Multidecadal Oscillation and its relation to rainfall and river flows in the continental U.S. *Geophysical Research Letters*, *28*(10), 2077-2080. doi: 10.1029/2000GL012745

Eyring, V., Bony, S., Meehl, G. A., Senior, C. A., Stevens, B., Stouffer, R. J., & Taylor, K. E. (2016). Overview of the Coupled Model Intercomparison Project Phase 6 (CMIP6) experimental design and organization. *Geosci. Model Dev.*, *9*(5), 1937–1958. doi: 10.5194/gmd-9-1937-2016

Fiedler, S., Kinne, S., Huang, W. T. K., Räisänen, P., O'Donnell, D., Bellouin, N., ... Lohmann, U. (2019a). Anthropogenic aerosol forcing – insights from multi-estimates from aerosol-climate models with reduced complexity. *Atmospheric Chemistry and Physics*, *19*, 6821–6841. doi: 10.5194/acp-19-6821-2019

Fiedler, S., Stevens, B., Gidden, M., Smith, S. J., Riahi, K., & van Vuuren, D. (2019b). First forcing estimates from the future CMIP6 scenarios of anthropogenic aerosol optical properties and an associated Twomey effect. *Geoscientific Model Development*, *12*, 989–1007. doi: 10.5194/gmd-12-989-2019

Fiedler, S., Stevens, B., & Mauritsen, T. (2017). On the sensitivity of anthropogenic aerosol forcing to model-internal variability and parameterizing a Twomey

effect. *J. Adv. Model. Earth Syst.*, *9*, n/a–n/a. doi: 10.1002/2017MS000932

Gervais, M., Shaman, J., & Kushnir, Y. (2018). Mechanisms Governing the Development of the North Atlantic Warming Hole in the CESM-LE Future Climate Simulations. *Journal of Climate*, *31*(15), 5927-5946. doi: 10.1175/JCLI-D-17-0635.1

Gervais, M., Shaman, J., & Kushnir, Y. (2019). Impacts of the North Atlantic Warming Hole in Future Climate Projections: Mean Atmospheric Circulation and the North Atlantic Jet. *Journal of Climate*, *32*(10), 2673–2689. doi: 10.1175/JCLI-D-18-0647.1

Gillett, N. P., Shiogama, H., Funke, B., Hegerl, G., Knutti, R., Matthes, K., ... Tebaldi, C. (2016). The Detection and Attribution Model Intercomparison Project (DAMIP v1.0) contribution to CMIP6. *Geoscientific Model Development*, *9*(10), 3685–3697. doi: 10.5194/gmd-9-3685-2016

Gryspeerdt, E., Mülmenstädt, J., Gettelman, A., Malavelle, F. F., Morrison, H., Neubauer, D., ... Zhang, K. (2020). Surprising similarities in model and observational aerosol radiative forcing estimates. *Atmospheric Chemistry and Physics*, *20*(1), 613–623. Retrieved from `https://acp.copernicus.org/articles/20/613/2020/` doi: 10.5194/acp-20-613-2020

IPCC. (2013). Annex v: Contributors to the ipcc wgi fifth assessment report [Book Section]. In T. Stocker et al. (Eds.), *Climate change 2013: The physical science basis. contribution of working group i to the fifth assessment report of the intergovernmental panel on climate change* (p. 1477–1496). Cambridge, United Kingdom and New York, NY, USA: Cambridge University Press. Retrieved from `www.climatechange2013.org` doi: 10.1017/CBO9781107415324

Jungclaus, J. H., Lohmann, K., & Zanchettin, D. (2014). Enhanced 20th-century heat transfer to the Arctic simulated in the context of climate variations over the last millennium. *Climate of the Past*, *10*(6), 2201–2213. doi: 10.5194/cp-10-2201-2014

Keil, P., Mauritsen, T., Jungclaus, J., Hedemann, C., Olonscheck, D., & Ghosh, R. (2020). Multiple drivers of the north atlantic warming hole. *Nature Climate Change*, *10*(7), 667–671. doi: 10.1038/s41558-020-0819-8

Kim, W. M., Yeager, S. G., & Danabasoglu, G. (2018). Key Role of Internal Ocean Dynamics in Atlantic Multidecadal Variability During the Last Half Century. *Geophysical Research Letters*, *45*(24), 13,449–13,457. doi: 10.1029/2018GL080474

Knight, J. R., Allan, R. J., Folland, C. K., Vellinga, M., & Mann, M. E. (2005). A signature of persistent natural thermohaline circulation cycles in observed climate. *Geophysical Research Letters*, *32*(20). doi: 10.1029/2005GL024233

Maher, N., Milinski, S., Suarez-Gutierrez, L., Botzet, M., Dobrynin, M., Kornblueh, L., ... Marotzke, J. (2019). The Max Planck Institute Grand Ensemble: Enabling the Exploration of Climate System Variability. *Journal of Advances in Modeling Earth Systems*, *11*(7), 2050-2069. doi: 10.1029/2019MS001639

Mauritsen, T., Bader, J., Becker, T., Behrens, J., Bittner, M., Brokopf, R., ... Roeckner, E. (2019). Developments in the MPI-M Earth System Model version 1.2 (MPI-ESM 1.2) and its response to increasing CO2. *Journal of Advances in Modeling Earth Systems*, *11*, 998–1038. doi: 10.1029/2018MS001400

Otterå, O. H., Bentsen, M., Drange, H., & Suo, L. (2010, 09). External forcing as a metronome for Atlantic multidecadal variability. *Nature Geoscience*, *3*, 688–694. doi: 10.1038/ngeo955

Pincus, R., Forster, P. M., & Stevens, B. (2016). The Radiative Forcing Model Intercomparison Project (RFMIP): experimental protocol for CMIP6. *Geoscientific Model Development*, *9*(9), 3447–3460. doi: 10.5194/gmd-9-3447-2016

Rahmstorf, S., Box, J. E., Feulner, G., Mann, M. E., Robinson, A., Rutherford, S., & Schaffernicht, E. J. (2015, 03). Exceptional twentieth-century slowdown in Atlantic Ocean overturning circulation. *Nature Climate Change*, *5*, 475 EP -.

Savitzky, A., & Golay, M. J. E. (1964). Smoothing and differentiation of data by simplified least squares procedures. *Analytical Chemistry*, *36*(8), 1627-1639. doi: 10.1021/ac60214a047

Stevens, B., Fiedler, S., Kinne, S., Peters, K., Rast, S., Müsse, J., ... Mauritsen, T. (2017). MACv2-SP: a parameterization of anthropogenic aerosol optical properties and an associated Twomey effect for use in CMIP6. *Geosci. Mod. Dev.*, *10*(1), 433–452. doi: 10.5194/gmd-10-433-2017

Trenberth, K. E., & Shea, D. J. (2006). Atlantic hurricanes and natural variability in 2005. *Geophysical Research Letters*, *33*(12). doi: 10.1029/2006GL026894

Wang, C., Dong, S., Evan, A. T., Foltz, G. R., & Lee, S.-K. (2012). Multidecadal Covariability of North Atlantic Sea Surface Temperature, African Dust, Sahel Rainfall, and Atlantic Hurricanes. *Journal of Climate*, *25*(15), 5404–5415. doi: 10.1175/JCLI-D-11-00413.1

Wild, M. (2009). Global dimming and brightening: A review. *Journal of Geophysical Research: Atmospheres*, *114*(D10). doi: 10.1029/2008JD011470

Zappa, G., Shaffrey, L. C., & Hodges, K. I. (2013). The Ability of CMIP5 Models to Simulate North Atlantic Extratropical Cyclones. *Journal of Climate*, *26*(15), 5379–5396. doi: 10.1175/JCLI-D-12-00501.1

Zhang, L., & Wang, C. (2013). Multidecadal North Atlantic sea surface temperature and Atlantic meridional overturning circulation variability in CMIP5 historical simulations. *Journal of Geophysical Research: Oceans*, *118*(10), 5772–5791. doi: 10.1002/jgrc.20390